X-921-74-131
PREPRINT

NASA TM X- 70709

GLOBAL DETAILED GEOID COMPUTATION AND MODEL ANALYSIS

JAMES G. MARSH
SAMIR VINCENT

MARCH 1974

GODDARD SPACE FLIGHT CENTER
GREENBELT, MARYLAND

For information concerning availability
of this document contact:

Technical Information Division, Code 250
Goddard Space Flight Center
Greenbelt, Maryland 20771

(Telephone 301-982-4488)

GLOBAL DETAILED GEOID COMPUTATION AND MODEL ANALYSIS

James G. Marsh
Geodynamics Branch
Earth Survey Applications Division
Goddard Space Flight Center
National Aeronautics and Space Administration
Greenbelt, Maryland, USA, 20771

and

Samir Vincent
Computer Sciences Corporation
8728 Colesville Road
Silver Spring, Maryland, USA, 20910

March 1974

ABSTRACT

This paper presents a survey of recent works on the gravimetric geoid. The gravity models considered have been those published in the past few years by the Goddard Space Flight Center (GSFC), the Smithsonian Astrophysical Observatory (SAO) and the Ohio State University (OSU). Comparisons and analyses have been carried out through the use of detailed gravimetric geoids which we have computed by combining the above-mentioned models with a set of 26,000 $1° \times 1°$ mean free air gravity anomalies. The accuracy of the detailed gravimetric geoid computed using the most recent Goddard Earth Model (GEM-6) in conjunction with the set of $1° \times 1°$ mean free air gravity anomalies is assessed at ±2 meters on the continents of North America, Europe and Australia, 2 to 5 meters in the North-East Pacific and North Atlantic areas and 5 to 10 meters in other areas where surface gravity data are sparse. R.M.S. differences between this detailed geoid and the detailed geoids computed using the other satellite gravity fields in conjuction with same set of surface data range from 3 to 7 meters. The maximum differences in all cases occurred in the Southern Hemisphere where surface data and satellite observations are sparse. These differences exhibited wavelengths of approximately 30° to 50° in longitude. Detailed geoid heights were also computed with models truncated to 12th degree and order as well as 8th degree and order. This truncation resulted in a reduction of the rms differences to a maximum of 5 meters. Comparisons have been made with the astrogeodetic

data of Rice (United States), Bomford (Europe), and Mather (Australia) and also with geoid heights from satellite solutions for geocentric station coordinates in North America and the Caribbean.

CONTENTS

ILLUSTRATIONS

ILLUSTRATION (continued)

ILLUSTRATION (continued)

ILLUSTRATION (continued)

TABLES

1. Introduction

This paper presents a survey of recent works on the gravimetric geoid, with particular reference to results obtained at Goddard Space Flight Center.

The geoid is the equipotential surface of the Earth's gravity field which most nearly corresponds to mean sea level, with the gravitational potential of the Earth consisting of both the attraction and rotation potentials. Since the distribution of material in the earth is irregular and the density varies, the force of gravity varies from place to place and the geoid is an irregular surface. The computation of surveys would be difficult on the geoid surface, therefore, an ellipsoid is adopted which best fits the geoid. The separation of the geoid above or below the reference ellipsoid is defined as the geoid height, the distance being taken along the normal to the ellipsoid.

Geoid heights can be computed two ways: (1) by the astrogeodetic method or, (2) by the gravimetric method, which is the subject of this paper. In the astrogeodetic method, the direction of the gravity vector is used in determining the shape of the geoid (deflection of the vertical). This is done by comparing the astronomic and geodetic coordinates of the same point on the surface of the Earth. This difference gives the slope of the geoid relative to the adopted ellipsoid. By arbitrarily fixing the geoid height at one point, the relative heights at other points can be determined by integrating the astrogeodetically determined slopes along profiles. The gravimetric method on the other hand, employs the magnitude of gravity utilizing potential theory. The magnitude of gravity can be measured

by surface techniques or from an analysis of satellite orbital perturbations. Astrogeodetic geoids can be very accurate (rms of ± 1 m) when a dense network of closely spaced deflection points exists. Practically all astrogeodetic geoid computations have been carried out on land areas due to the difficulties in maintaining a stable platform at sea. This fact, coupled with the high level of success in determining the long wave length components of the Earth's gravity field from satellite observations prompted the use of gravimetric methods for the determination of global geoids. Regional geoids, however, are still being determined by astrogeodetic techniques. This latter fact is well illustrated by the recent astrogedetic computations carried out by Rice (1973a) in the continental United States, Vaníček and Merry (1973) and Lachapelle (1973) in Canada, Bomford (1972) in Western Europe, Mather, et al. (1971) in Australia and Fischer (1967) in North and Central America.

The early gravimetric geoid computations of Hirvonen (1934), Tanni (1948, 1949), Heiskanen (1957) and Kivioja et al (1966), were based solely on surface gravity data. All of these pre-satellite geoids suffered from a lack of worldwide gravity coverage. With the advent of satellites it has been possible to derive the long wavelength components of the gravity field on a worldwide basis with considerable accuracy. The most recent satellite determinations of the Earth's gravity field have been the Smithsonian Astrophysical Observatory (SAO) Standard Earth Models 2 and 3 (Gaposchkin and Lambeck, 1970), (Gaposchkin, 1973), the Goddard Earth Models (GEM) 4, 5, and 6, (Lerch et al. 1972, 1974), and the Ohio State University (OSU) Model (Rapp, 1974). Recently, efforts have

been undertaken at Goddard to combine the satellite derived gravity data with $1° \times 1°$ mean values of surface gravity data to provide more accurate estimates of the geoidal undulations. The results of this latter effort comprise the major portion of this paper.

In the process of computing the combination geoids, several satellite gravity models published in the past four years were tested in order to determine the best gravity model for detailed geoid computations. The satellite models used in the geoid computations were those mentioned above. The rms differences between geoid heights computed using the GEM-6 gravity model and those computed using other gravity models ranged from 3 meters for the Rapp 1974 model to 7 meters for the SAO-3 gravity model when the computations utilized the complete set of spherical harmonic coefficients.

The largest geoid height differences occurring in the above comparisons were located in the Southern Hemisphere. These differences exhibited a wavelength of approximately 30° in longitude. Geoid profiles at 10° intervals in latitude were compared for all models. Differences between the geoids along these profiles were generally 5 meters in areas of relatively dense surface gravity data and as large as 25 meters in areas of sparse or absent surface gravity data.

An accurate knowledge of the geoid is becoming increasingly important for geodetic and geophysical applications. For example, a global resolution of ±5 m in geoid height provides useful detailed information concerning the shape of the

geoid. This can serve as an independent means of comparison with astrogeodetic data over the continents in terms of information relative to the accuracy of the geoid undulations and geodetic datum orientation. A geoid with this resolution can also be used as a height constraint on global geodetic satellite solutions for the coordinates of tracking stations. A resolution of +10 cm is of fundamental importance to physical oceanographers in that the measurement of the difference between the sea surface topography and the geoid would be practical. This latter comparison would permit detection of tides on continental shelves, storm surges and currents.

A contour map of the detailed gravimetric geoid computed using the GSFC GEM-6 Model is presented in this paper. The accuracy of this geoid is considered to be ±2 meters on the continents of North America, Europe and Australia, 2 to 5 meters in the North East Pacific and Atlantic areas and 5 to 10 meters in other areas where surface gravity data are sparse. The accuracy of the detailed geoid in land areas was established by comparing the detailed gravimetric geoid with the astrogeodetic geoids of; Rice in the United States, Bomford in Europe and Mather in Australia. In the ocean areas, the accuracy of the detailed geoid was a function of the amount and quality of the surface gravity data.

2. Principles of Computation

The geoidal undulation at any point P on the Earth can be computed using the well known Stokes' formula:

$$N(\phi, \lambda) = \frac{R}{4\pi\bar{\gamma}} \int_{\lambda'=0}^{2\pi} \int_{\phi'=-\pi/2}^{\pi/2} \Delta g_T(\phi', \lambda') \, S(\Psi) \cos\phi' \, d\phi' \, d\lambda' \qquad (1)$$

where

ϕ, λ = the geocentric latitude and longitude, respectively, of the computation point.

ϕ', λ' = the geocentric latitude and longitude, respectively, of the variable integration point.

$N(\phi, \lambda)$ = geoid undulation at ϕ, λ.

R = mean radius of the Earth.

$\bar{\gamma}$ = mean value of gravity over the Earth.

$\Delta g_T(\phi', \lambda')$ = free air gravity anomaly at the variable point ϕ', λ'.

$$S(\Psi) = \frac{1}{\sin(\Psi/2)} - 6\sin(\Psi/2) + 1 + 5\cos\Psi - 3\cos\Psi \ln(\sin(\Psi/2) + \sin^2(\Psi/2)) \qquad (2)$$

where

$$\Psi = \cos^{-1}[\sin\phi \sin\phi' + \cos\phi \cos\phi' \cos(\lambda - \lambda')] \qquad (3)$$

Hirvonen (1934) calculated the geoidal undulations for 62 points distributed in an east-west band encircling the surface of the Earth using Stokes' formula.

Tanni (1948, 1949) computed geoidal heights using Stokes' formula as Hirvonen did, but with a larger amount of gravity data. Tanni computed global undulations using $5° \times 5°$ blocks and a more detailed geoid for Europe using $1° \times 1°$ blocks. Heiskanen (1957) computed a geoid based upon 6679 $1° \times 1°$ mean free air anomalies. Kivioja et al (1966) computed a global geoid map using Stokes' formula for 2592 $5° \times 5°$ surface elements. All these pre-satellite geoids lacked global coverage of observed gravity data.

With the advent of artifical satellites, analyses of orbital perturbations have yielded spherical harmoic coefficients for the representation of the Earth's gravity field. Given a set of harmonic coefficients $\bar{C}_n^m$, $\bar{S}_n^m$ a number of methods exist for the computation of the geoid undulations. The method we have used consists of fixing a value of the potential, W_0, and computing the geoid height, N, as

$$N = r - r_E \tag{4}$$

where

r is the radial distance to the equipotential surface defined by W_0 and the potential coefficients of the gravitational potential model.

r_E is the radial distance to a selected reference-ellipsoid defined by a semimajor axis (a_e) and flattening (f).

The radial distance r, to the equipotential surface W_0 at a particular latitude and longitude ϕ, λ is determined by using iteration techniques to solve equation (5) where the only unknown is r.

$$W_0 = \frac{GM}{r}\left[1 + \sum_{n=2}^{k}\sum_{m=0}^{n}\left(\frac{a_e}{r}\right)^n (\bar{C}_{nm}\cos m\lambda + \bar{S}_{nm}\sin m\lambda)\,\bar{P}_{nm}(\sin\phi)\right] + \frac{\omega^2 r^2}{2}\cos^2\phi \tag{5}$$

where

GM = the product of the gravitational constant and the mass of the Earth

a_e = semimajor axis of the reference ellipsoid

r = geocentric radius

ω = Earth's angular velocity

$\bar{C}_{nm}$ and $\bar{S}_{nm}$ = fully normalized spherical harmonic coefficients of the gravitational potential

$\bar{P}_{nm}(\sin\phi)$ = Normalized Associated Legendre Polynomial

In order to provide a more accurate representation of the geoid undulations, particularly with respect to the wavelengths shorter than those resolvable with satellite observations, we have combined the satellite derived gravity data with surface $1° \times 1°$ mean, free air gravity anomaly observations. In order to do so, the Earth was divided into two areas, a local area (A_1) surrounding the point P, and the remainder of the Earth (A_2). The anomalous gravity was partitioned into two parts, represented by the symbols Δg_s and Δg_2. The Δg_s values are defined as that part of the anomalous gravity field which can be represented by the coefficients in a satellite derived, spherical harmonic

expansion of the gravitational potential. The Δg_2 values are defined as the remainder of the anomalous gravity field. Using the division of the Earth's surface into two areas and of the anomalous gravity into two components one can write Equation 1 in the form:

$$N(\phi, \lambda) = N_1 + N_2 + N_3, \tag{6}$$

where

$$N_1 = \frac{R}{4\pi\bar{\gamma}} \int_0^{2\pi} \int_{-\pi/2}^{\pi/2} \Delta g_s(\phi', \lambda') S(\Psi) \cos \phi' \, d\phi' \, d\lambda',$$

$$N_2 = \frac{R}{4\pi\bar{\gamma}} \iint_{A_1} \Delta g_2(\phi', \lambda') S(\Psi) \cos \phi' \, d\phi' \, d\lambda', \tag{7}$$

$$N_3 = \frac{R}{4\pi\bar{\gamma}} \iint_{A_2} \Delta g_2(\phi', \lambda') S(\Psi) \cos \phi' \, d\phi' \, d\lambda'$$

For the computations described in this paper, the area A_1 for a point at which the geoid was being computed, was defined to consist of a twenty degree-by-twenty degree area centered on the computation point. Also in the calculations described here, the term N_3 in equation (6) was set equal to zero. This is equivalent to assuming that the satellite derived approximation to the gravity field is adequate for the area A_2 at a distance of greater than 10° from the computation point. This technique has been employed previously by a number of other investigators, e.g., Khan and Strange (1966) and Rapp (1967).

The parameters used in these computations were:

W_0 = the potential of the geoid
(62 636 875 m^2/s^2)

$\bar{\gamma}$ = the mean value of gravity
(9.789 m/s^2)

a_e = the semi-major of the reference ellipsoid
(6 378 142 m)

1/f = the flattening coefficient for the reference ellipsoid
(298.255)

GM = the product of the universal gravitational constant and the mass of the earth (3.986 009 $\times 10^{14}$ m^3/s^2)

ω = the rotation rate of the earth
(0.72 921 151 $\times 10^{-4}$ rad/s)

3. SATELLITE GRAVITY MODELS AND SURFACE DATA

3.1 Satellite Gravity Models

As mentioned earlier, detailed geoids were computed using the GSFC GEM-4 and 6, the SAO-2, and 3, and the Rapp 1974 satellite gravity models. A brief description of these models follows.

GEM 4 (Lerch et al, 1972) is a combination solution consisting of (1) a satellite solution designated GEM 3 based upon 400,000 optical, laser, and electronic observations on 27 satellites including low inclination data from SAS and PEOLE, and (2) 1707 5°-by-5° equiangular mean gravity anomalies based on 21,000 1°-by-1° surface gravity observations. The GEM 4 model is complete to degree and order 16 with additional terms to degree 22.

GEM 6 (Lerch et al, 1973) is a combination model consisting of (1) a satellite solution designated GEM 5 and (2) Rapp's 5° equal area mean gravity anomalies based on 26,000 1°-by-1° surface gravity values. GEM 6 is complete to degree and order 16 with additional terms to degree 22.

SAO 2 (Gaposchkin and Lambeck, 1970) is a combination model consisting of (1) a satellite solution based on optical and laser data obtained from 21 satellites and (2) 935 5°-by-5° equal area gravity anomalies derived by Kaula (1966). This model is complete to degree and order 16 with additional terms to degree 22.

SAO 3 (Gaposchkin, 1973) is a combination model consisting of (1) a satellite solution based on optical, laser, and Deep Space tracking data obtained from 25 satellites and (2) a set of surface gravity data similar to that of the SAO II model. This model is complete to degree and order 18 with additional zonal terms to degree 36 and resonant terms to degree 24.

Rapp 1974 is a combination model consisting of (1) a satellite solution GEM3 and (2) 1283 5°-by-5° equal area anomalies based on 23,355 1° × 1° surface gravity anomalies. This model is complete to degree and order 20 with additional terms to degree 22.

3.2 Surface Gravity Data

The surface gravity data used in the computations consisted primarily of 23,947 records of 1°-by-1° mean free air gravity anomalies obtained from the Defense Mapping Agency/Aerospace Center. This data set was complemented with collections from the National Ocean and Atmospheric Agency and the Hawaii

Institude of Geophysics. Where possible, data collected by local agencies were considered first in data-preparation. When these data were not sufficient, the above-mentioned sources were used to fill in the voids. The total set of surface data consisted of about 26,000 $1° \times 1°$ mean free air gravity anomalies. The data file is discussed in detail in Vincent et. al., 1973.

4. ANALYSIS

The satellite derived gravity model used in the detailed geoid computations provides information on the long wavelength (approximately $\geq$ 1000 km) undulations of the geoid. Short wavelength information is provided by the 1°-by-1° surface gravity data. All models tested were complete to degree and order 16 with selected higher degree terms and were therefore capable of providing the 1000 km information on the geoidal undulations. Since all models were combined with the same set of 1°-by-1° surface gravity data, the resultant differences in the detailed geoid heights are due to variations in the satellite gravity models. The analyses of the satellite models and the final choice of the best model for use in detailed geoid computations were carried out by 1) inter-comparing the respective geoids of these models, and 2) comparison with external standards such as astrogeodetic geoids and dynamically derived tracking station coordinates.

4.1 Inter-Model Comparisons

Detailed geoids were computed using the full sets of coefficients of the five gravity models and profiles were drawn along parallels of latitude around the

globe at 10° intervals in latitude. Figures 1 through 5 present representative examples of these profiles. In the Northern Hemisphere, profiles were chosen at 20° and 40° North latitude (Figures 1, 2). These profiles show an average variability of about ±5 meters, however, individual differences as large as 10 meters do appear. For example, in Figure 2 at longitude 180°E, the geoid computed using the SAO-2 model differs from the geoid computed using GEM-6 by 10 meters. The models show the largest scatter at 180°E mainly because of a lack of surface gravity data in this region. The dominant differences in these profiles are the amplitudes of the main features rather than the slopes of the geoids. It is noted that there are many places along these profiles where the respective geoid slopes vary by only a few percent.

In Figures 3 through 5 (Southern Hemisphere) a completely different picture emerges. The scatter is much larger. This is largely attributed to the sparsity of surface gravity data as well as a lack of satellite observational data in this part of the world. The scatter in the profiles increases gradually towards the Antarctic. For example, in Figure 3, the scatter is evident only along longitudes 200°E to 350°E, but in Figures 4 and 5 the divergence is noted along the entire length of the profile. In Figure 5, the maximum difference reaches approximately 25 meters at longitude 180°E. In contrast to the Northern Hemisphere, the geoid slopes in the Southern Hemisphere exhibit variations.

Contour maps were also prepared for the differences between GEM-6 and the other models. Analysis of these contour maps revealed that the geoid height

differences in many areas exhibited a wavelength of 30° to 50°. This variation, when translated into spherical harmonic terms, corresponds to about the 9th degree and order. The orbital perturbations arising from spherical harmonic coefficients of degree and order larger than 8, 8 are generally on the order of a few meters, a fact which makes an accurate recovery of the individual coefficients values difficult except in the case of resonance. Brownd, et al., 1973 found that when satellite derived gravity anomalies were compared with surface gravity data using truncated models, the (12, 12) field agreed best with the surface data while the lower and the higher degree models were divergent from the surface data. The results of the above analysis coupled with the scarcity of surface gravity data in the southern Hemisphere led to recomputation of the detailed geoids using gravity models truncated to (12, 12) and (8, 8).

Figures 6 through 10 present profiles of detailed geoids computed using models truncated at (12, 12) plus SAO-2, and -3 truncated at 8, 8. One point noted throughout these profiles is that truncation at (12, 12) for the GEM-4, -6 and Rapp '74 models generally reduces the differences among them to an envelope of about 2 meters. The SAO-2 and -3 (12, 12) models on the other hand show variations at large as 5 meters with respect to each other. They also are in disagreement with the general trend of the other truncated models in some areas, as well as indicating features not portrayed by the general trend. For example, at 175° longitude in Figure 9 the SAO-3 profile appears to be shifted by about 15° in longitude with respect to the other models. However, further

truncation of the SAO-2, and -3 models to (8, 8) generally reduces the differences along the main features and eliminates some of the extraneous features. Thus, as the models are truncated, the results of the geoid computations tend to come into better agreement. This is undoubtedly due to the fact that the lower degree and order coefficients in all models are more accurately determined.

RMS differences have also been calculated for the complete and truncated models versus GEM-6. A summary of these differences is presented below.

GEM-6 vs.	COMPLETE MODEL	MODELS TRUNCATED AT (12, 12)
Rapp	±2.7m	±1.6m
GEM-4	±3.7m	±1.3m
SAO-2	±4.5m	±3.3m
SAO-3	±6.5m	±5.2m

It is noted that these differences are relative and that they should not be used as a measure of the absolute accuracy of the geoid. Global rms differences, while of interest, may not be representative since the differences in the Southern Hemisphere are much larger than in the Northern Hemisphere.

Figures 11 through 14 present the geoid height differences in histogram form. The most frequent differences are in the range of +5 to -5 meters. The histograms also display the better agreement of the truncated models.

4.2 Comparison with External Standards

4.2.1 Comparisons with Astrogeodetic Geoids

Detailed gravimetric geoids computed with the above mentioned models were compared with the astrogeodetic geoids of Bomford (1971) in Europe, Rice (1973b)

in the United States, and Mather et al. (1971) in Australia. In all cases, the astrogeodetic geoids were transformed to a center of mass system using transformation parameter values of Marsh, et al. (1973) before comparisons were made.

In Europe, due to the availability of 1°-by-1° data, we were able to compute detailed gravimetric geoids with the Stokes' function integrated 20° around the computation point, in addition to the usual 10° integration. This was done as a means of assessing the long wavelength contributions of the gravity models since the geoid based upon a 20° integration would be less sensitive to long wavelength errors in the satellite gravity model. A profile at latitude 48°N, recommended by Bomford as being the most representative, was used for the comparison. The SAO-2 and -3 profiles were similar, but they were different from those for the GEM-4, -6, and the Rapp 74 models. In the case of the 10° integration, the detailed geoid using the SAO-3 model showed a tilt of 1.6 arc seconds with respect to the astrogeodetic geoid. However, when the GEM-6 model was used, the differences became much less systematic and were on the order of ±2 meters (Figure 15). When the 20° integration was performed, the SAO-3 detailed geoid rotated by more than one arc second while the GEM-6 detailed geoid changed by a much smaller amount, with both profiles now agreeing well with the astrogeodetic geoid. The results of this test indicated that the GEM-6 model represented the long wavelength features more accurately in this area (Figure 16). Similar comparisons were carried out in the area of North America, with the result that little change was noted when the integration was carried out to 20° versus 10°.

In Australia, the comparisons with Mather's astrogeodetic geoid were conducted along a profile 26° South (Figure 17). The detailed geoid, when based upon the SAO-3 model, exhibited a tilt of 1 arc second with respect to Mather's geoid. However, the detailed geoid based upon the GEM-6 model showed only 0.5 arc second tilt. GEM-6 matched the results Mather found in his studies on the Australian datum.

Another comparison was made with Rice's astrogeodetic geoid along a profile in the U.S. at latitude 35°N. Table I presents the differences between Rice's geoid and detailed geoids computed by using the various models. The agreement between Rice's geoid and all the models along this profile was on the order of ±2 meters.

4.2.2 Comparison with Dynamic Station Heights – Goddard Space Flight Center Long-Arc Orbital Analyses have provided geocentric coordinates for tracking stations (Marsh et al., 1973). Geoid heights of the tracking stations derived from this solution were compared with the detailed geoid heights. Table II presents the results of these comparisons for stations in the U.S. and in the Caribbean. The results obtained using the satellite models are similar except for those computed using the SAO-3 model where differences as large as 5 meters versus the average are apparent. The rms agreement for all models is about ±3 meters. This agreement is considered excellent, considering the various error sources inherent in this type of comparison. For, example, errors can be attributed to:

a. Dynamically derived station heights

b. Surveyed heights above mean sea level and the definition of mean sea level

c. Gravimetric geoid heights

5. THE GODDARD EARTH MODEL (GEM-6) DETAILED GEOID

As a result of the previously discussed tests and comparisons, GEM-6 was adopted as the base model for the computation of a global detailed gravimetric geoid contour map which is included in this paper. This contour map is presented in Figure 18. The constants presented earlier were used in this computation. The differences between this detailed geoid and a geoid based solely upon the GEM-6 coefficients are generally less than 15 meters. For example, in Australia prominent differences of 10 to 12 meters occur in the eastern parts of the country, due to the dominance of mountain ranges that adjoin relatively flat plains and shallow continental slopes. A difference of 15 meters is noted over the Puerto Rico Trench. This is caused by a large gravity gradient over a region which is small compared to the resolution of the GEM-6 model. These differences are the representation of the surface gravity short wavelength contributions to the geoid which are not provided by the GEM-6 model.

6. SUMMARY

The accuracy of the GEM-6 detailed geoid, presented in this paper, is assessed as ±2 meters in areas of dense surface gravity coverage.

The greatest divergences in the models appeared in areas of sparse surface data coverage, notably in the Southern Hemisphere. The magnitude of these differences was as large as 25 meters with a wavelength of approximately 30° to 50°. This indicates that caution should be exercised in interpreting geoidal details provided by higher degree and order harmonic coefficients when surface data is lacking.

A general lack of surface gravity data, especially in the Southern Hemisphere, is a limiting factor in present detailed global computations of the geoid. Currently, less than 40% of the globe is covered with $1° \times 1°$ surface gravity data. This deficiency is also compounded by the fact that the majority of the satellite tracking stations are located in the Northern Hemisphere, with few stations located beyond 50° North or South latitude.

It is anticipated that the distribution of satellite observational data will be enhanced greatly with the implementation of a new tracking technique, called Satellite-to-Satellite Tracking (SST), planned for the future. SST consists basically of using a satellite in a high stable orbit to track a lower altitude satellite in an orbit highly perturbed by the Earth's gravity field. The main advantage of this new technique over current techniques is that extensive tracking coverage, both geographically and in time, will be possible. The first experiments using this technique are the ATS-F/NIMBUS-E and ATS-F/GEOS-C Experiments, planned for the fall of 1974.

A new technique for the determination of geoidal undulations in ocean areas is also currently being evaluated. This technique involves the use of an orbiting radar altimeter to measure the sea surface to satellite distance. One of the recent SKYLAB Earth Resources Experiments involved the use of a radar altimeter. Data from this experiment have been compared with a Goddard detailed gravimetric geoid in the Altantic Ocean area (McGoogan, 1974). The preliminary results of these comparisons are excellent and promote the use of satellite altimeters.

The GEOS-C satellite to be launched in the Fall of 1974 will also carry a radar altimeter capable of providing data with a precision of ±1 meter. The GEOS-C altimeter will provide a 5° spatial resolution. Even though the primary objective of the GEOS-C altimetry experiment is to further establish the feasibility of satellite-borne altimetry, this will be the first step in a series of satellite altimetry missions for the collection of a global set of data for the direct study of the geoid and ocean surface.

ACKNOWLEDGMENT

The authors acknowledge the very helpful discussions and suggestions of William E. Strange of Computer Sciences Corporation.

REFERENCES

Bomford, G., 1972, "The Astro-Geodetic Geoid in Europe and Connected Areas," Report for Study Group V-29, 15th Gen. Assemb., IUGG, 1971, Moscow, USSR, in Travaux de l'association Internationale de Geodésie, 24, pages 357-371, Paris.

Brownd, G., and Richardson, J. A., 1973, Computer Sciences Corporation, personal communication.

Fischer, I., 1967, "Geoid Charts of North and Central America," Technical Report 62, Army Map Service, Washington, D. C.

Gaposchkin, E. M., and Lambeck, K., 1970, "Smithsonian Standard Earth (II)," Smithsonian Astrophysical Observatory, Special Report 315.

Gaposchkin, E. M., 1973, "Smithsonian Standard Earth III," presented at the American Geophysical Union Meeting, Washington, D. C.

Heiskanen, W. A., 1957, "The Columbus Geoid," Transactions AGU, Volume 38, pages 841 to 848.

Hirvonen, R. A., 1934, "The Continental Undulations of the Geoid," Publication No. 19, Finnish Geodetic Institute.

Kaula, W. M., 1966, "Tests and Combination of Satellite Determinations of the Gravity Field with Gravimetry," Journal of Geophysical Research, Volume 71, pages 5303 to 5314.

Khan, M. A., Strange, W. E., 1966, "Investigations on the Shape of the Geoid in North America," (Abstract) Transactions AGU, Volume 47, Number 1.

Kivioja, L. A., Lewis, A. D. M., 1966, "Free Air Gravity Anomalies Caused by the Gravitational Attraction of Topographic, Bathymetric Features, and Their Isostatic Compensating Masses and Corresponding Geoid Undulations," AGU Geophysical Monograph No. 9, pages 89 to 95.

Lachapelle, G., 1973, "A Study of the Geoid in Canada," Geoidetic Institute, Helsinki, Finland, Private Communication.

Lerch, F., et al., 1971, "Gravitational Field Models GEM-3 and GEM-4," Goddard Space Flight Center Document Number X-592-72-476, Greenbelt, Maryland.

Lerch, F., et al., 1973, "Gravitational Field Models GEM-5 and GEM-6," Goddard Space Flight Center Contribution to the National Geodetic Satellite Program Final Report.

Marsh, J. G., Douglas, B. C., Klosko, S. M., 1973, "Global Station Coordinates Solution Based upon Camera and Laser Data – GSFC 1973," Paper presented at the First International Symposium, The Use of Artificial Satellites for Geodesy and Geodynamics, Athens, Greece; also GSFC Document X-592-73-171.

Mather, R. S., Barlow, B. C., Fryer, J. G., 1971, "The Australian Geodetic Datum in Earth Space," Unisurv Report No. 22, University of New South Wales, Australia.

McGoogan, J. T., 1974, "Precision Satellite Altimetry", Paper presented at the Institute of Electrical and Electronics Engineers, International Convention and Exposition, March 26-29, Session 34.

Rapp, R. H., 1967, Combination of Satellite and Terrestrial Data for a Detailed Geoid," (Abstract) EOS Transactions, AGU, Volume 48, Number 54.

Rapp, R. H., 1974, "The Earth's Gravitational Field from the Combination of Satellite and Terrestrial Data," Paper presented at the Symposium on Earth's Gravitational Field and Secular Variations in Position, Sydney Australia, Nov. 1973, (in press).

Rice, D. A., 1973a, "Frame of Reference for the New Adjustment of the North American Datum," EOS Transactions, AGU, Volume 54, Number 11.

Rice, D. A., 1973b, National Ocean Survey, Personal Communication.

Tanni, L., 1948, "On the Continental Undulations of the Geoid as Determined from the Present Gravity Material," Publication No. 18, Isostatic Institute, International Association of Geodesy, Helsinki.

Tanni, L., 1949, "The Regional Rise of the Geoid in Central Europe," Publication No. 22, Isostatic Institute, International Association of Geodesy, Helsinki.

Vaníček, P., Merry, C. L., 1973, "Determination of the Geoid from Deflections of the Vertical Using a Least-Squares Surface Fitting Technique," Canadian Federal Department of Energy, Mines and Resources, Surveys and Mapping Branch, Private Communication.

Vincent, S., and Marsh, J. G., 1973, "Global Detailed Gravimetric Geoid," Paper presented at the First International Symposium, The Use of Artifical Satellites for Geodesy and Geodynamics, Athens, Greece; also GSFC Document X-592-73-266.

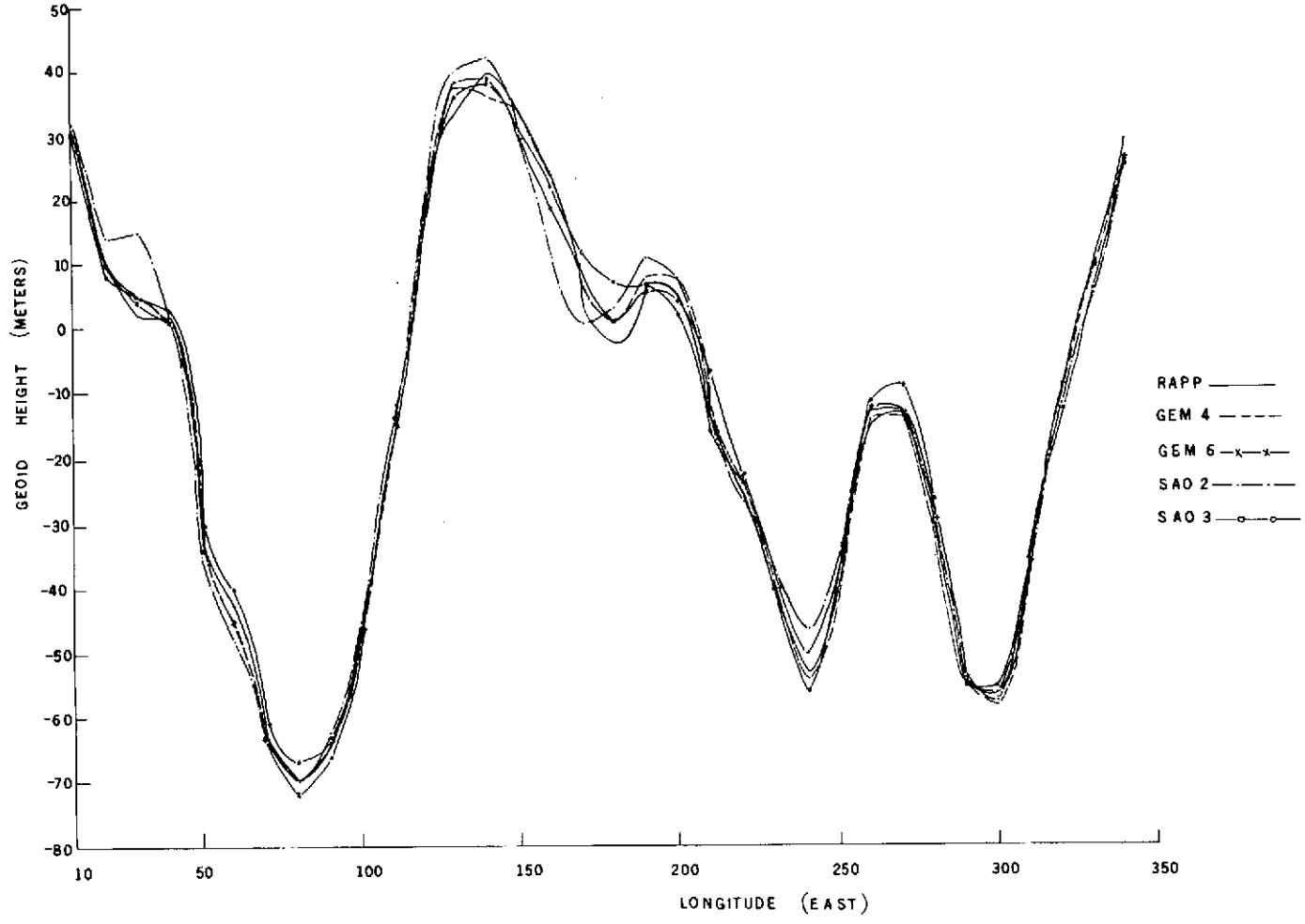

Figure 1. Detailed geoid height profiles at 20°N latitude, based upon the Rapp, GEM-4, GEM-6, SAO-2 and SAO-3 models. The general agreement is on the order of 5 meters. In the areas of 100° to 150° and 300° to 350°E longitude the agreement as to the slope of the geoid is good, however at 50° and 175°, differences as large as 10 meters are noted.

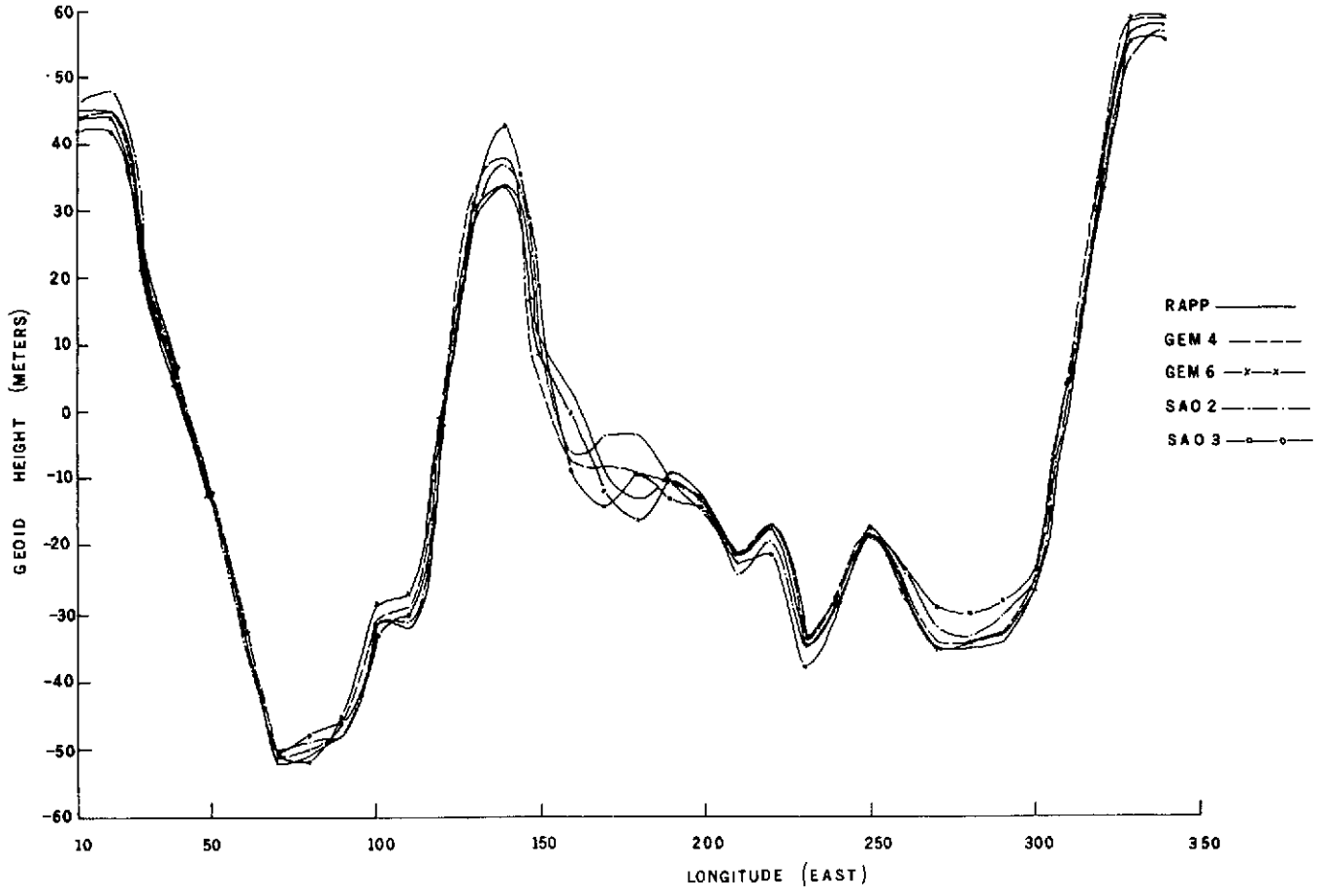

Figure 2. Detailed geoid height profiles at 40°N latitude based upon the models indicated. This figure is similar to Figure 1 except that now between 150° and 300° the differences are larger. This is attributed to the sparsity of satellite and surface data in this area.

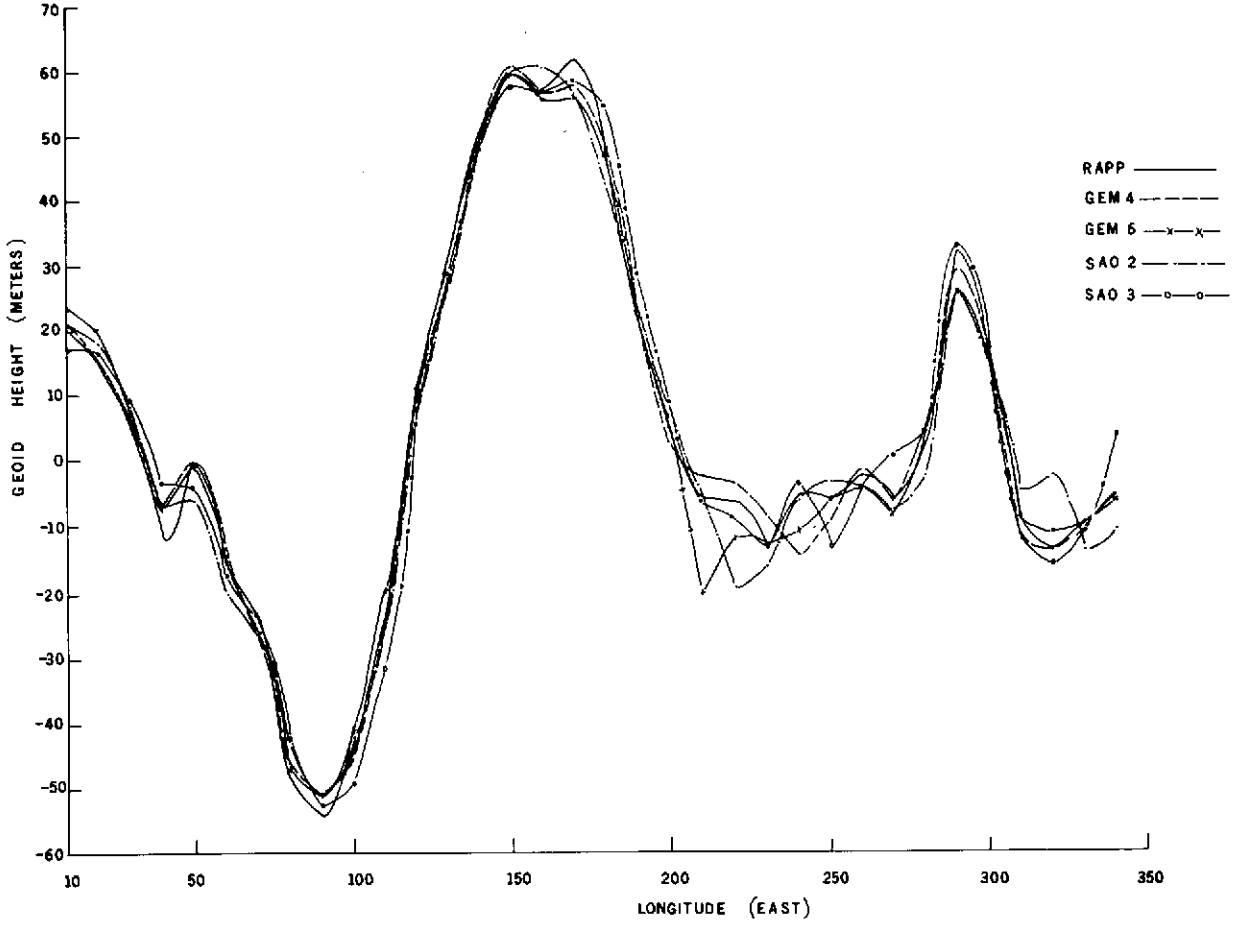

Figure 3. Detailed geoid height profiles at 20°S latitude based upon the models indicated. Although the agreement is still good in the area of 100° to 150°E longitude, a further degradation is noted in the area of 200° to 275°E longitude.

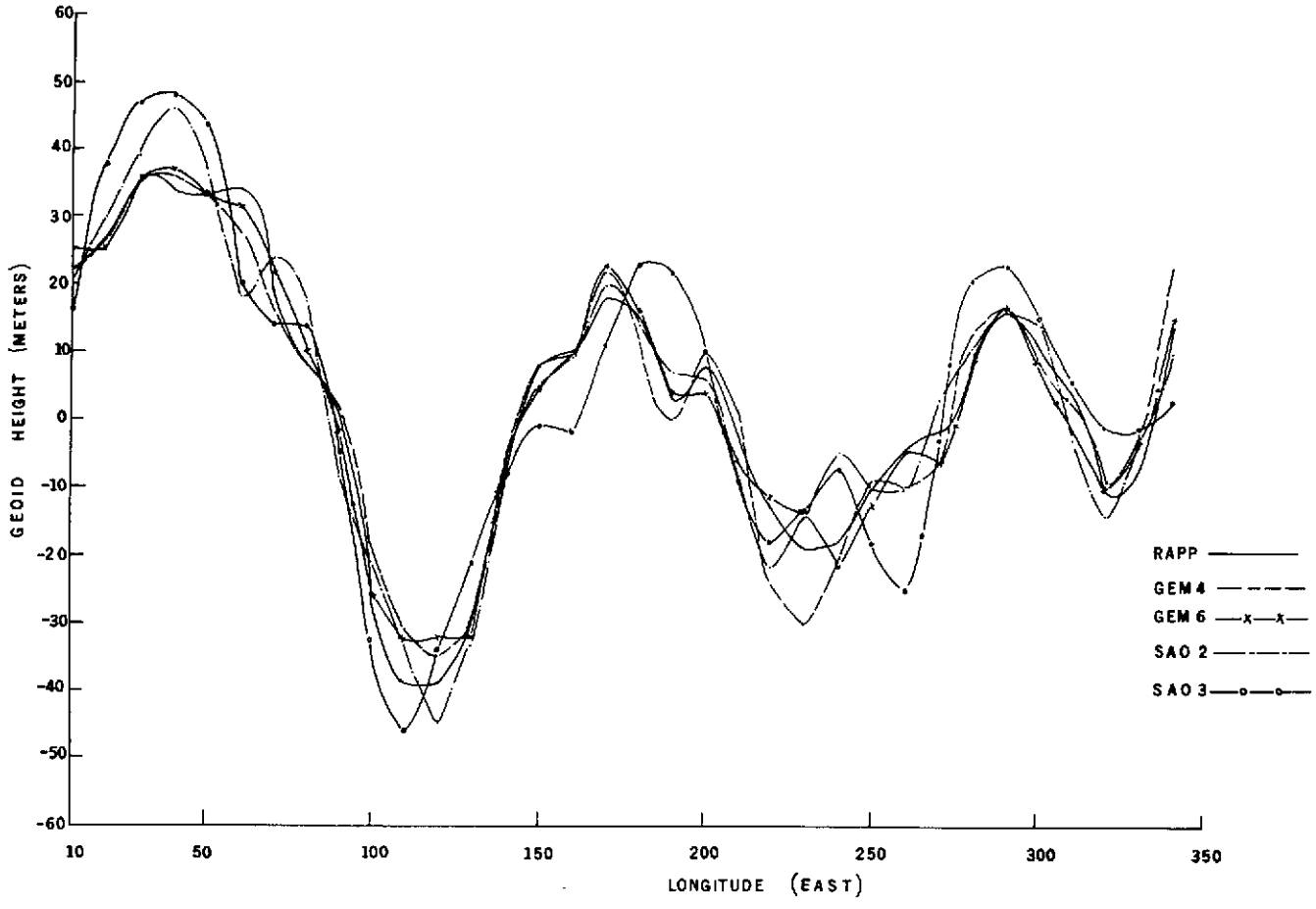

Figure 4. Detailed geoid height profiles at 40°S latitude based upon the models indicated. The differences are generally on the order of 10 meters. In some places, features indicated by one model do not conform to the general trend indicated by the other models, for example, at 225° for GEM-4 and at 260° for SAO-3.

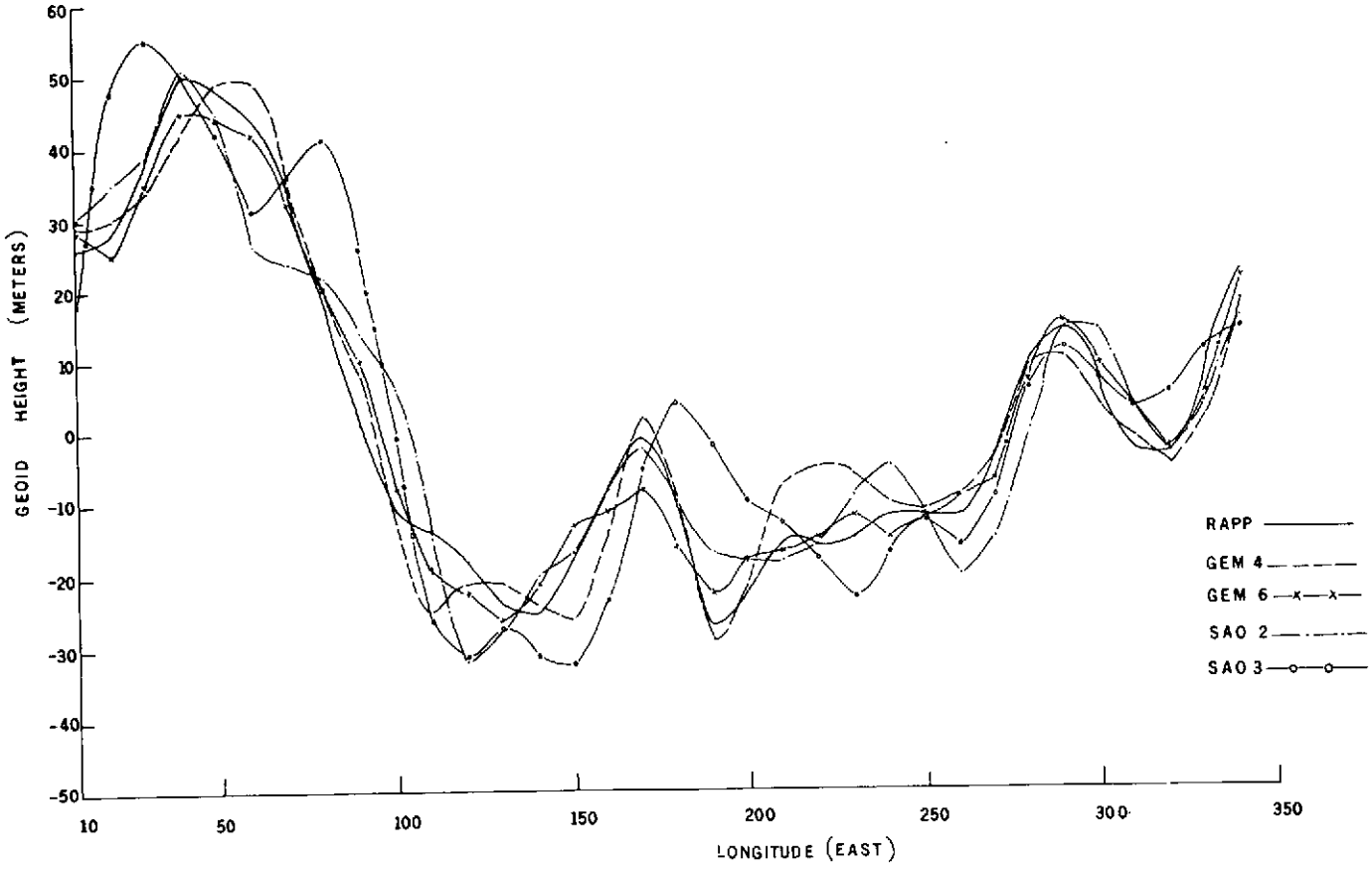

Figure 5. Detailed geoid height profiles at 50°S latitude based upon the models indicated. The general agreement is much poorer than indicated in the previous figures at higher latitudes. Differences as large as 25 meters are noted, also some features are displaced by as much as 25°. These large differences reflect the lack of satellite and surface observational data at lower latitudes.

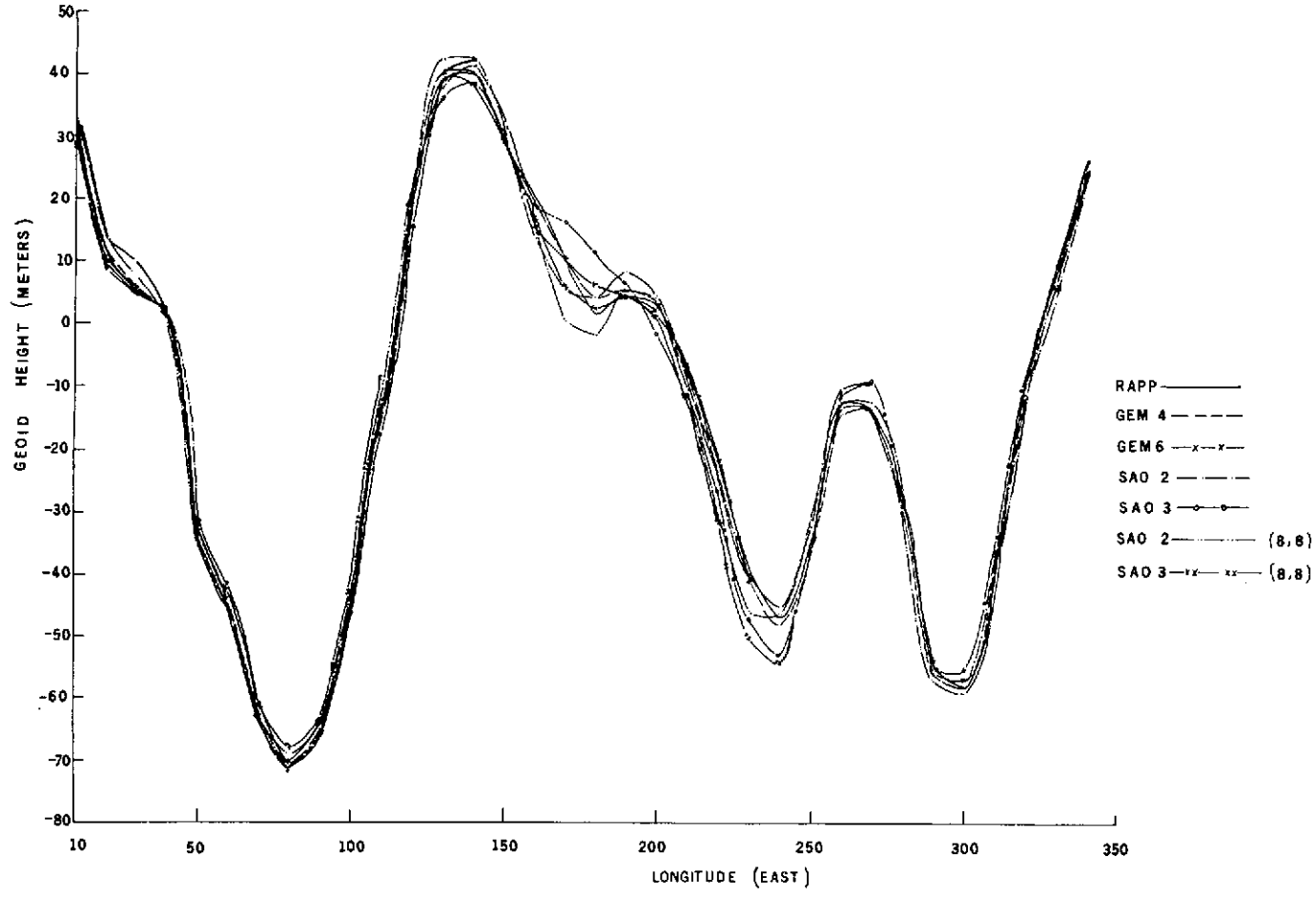

Figure 6. Detailed geoid height profiles at 20°N latitude based upon the models indicated. All models have been truncated at degree and order 12. In addition, profiles are presented for the SAO models truncated at (8, 8). The general agreement is on the order of 5 meters except at 175°. At this longitude, truncation of the SAO-3 model to (8, 8) produced better agreement with the general trend, however, further truncation of the SAO-2 model resulted in a deviation from the general trend.

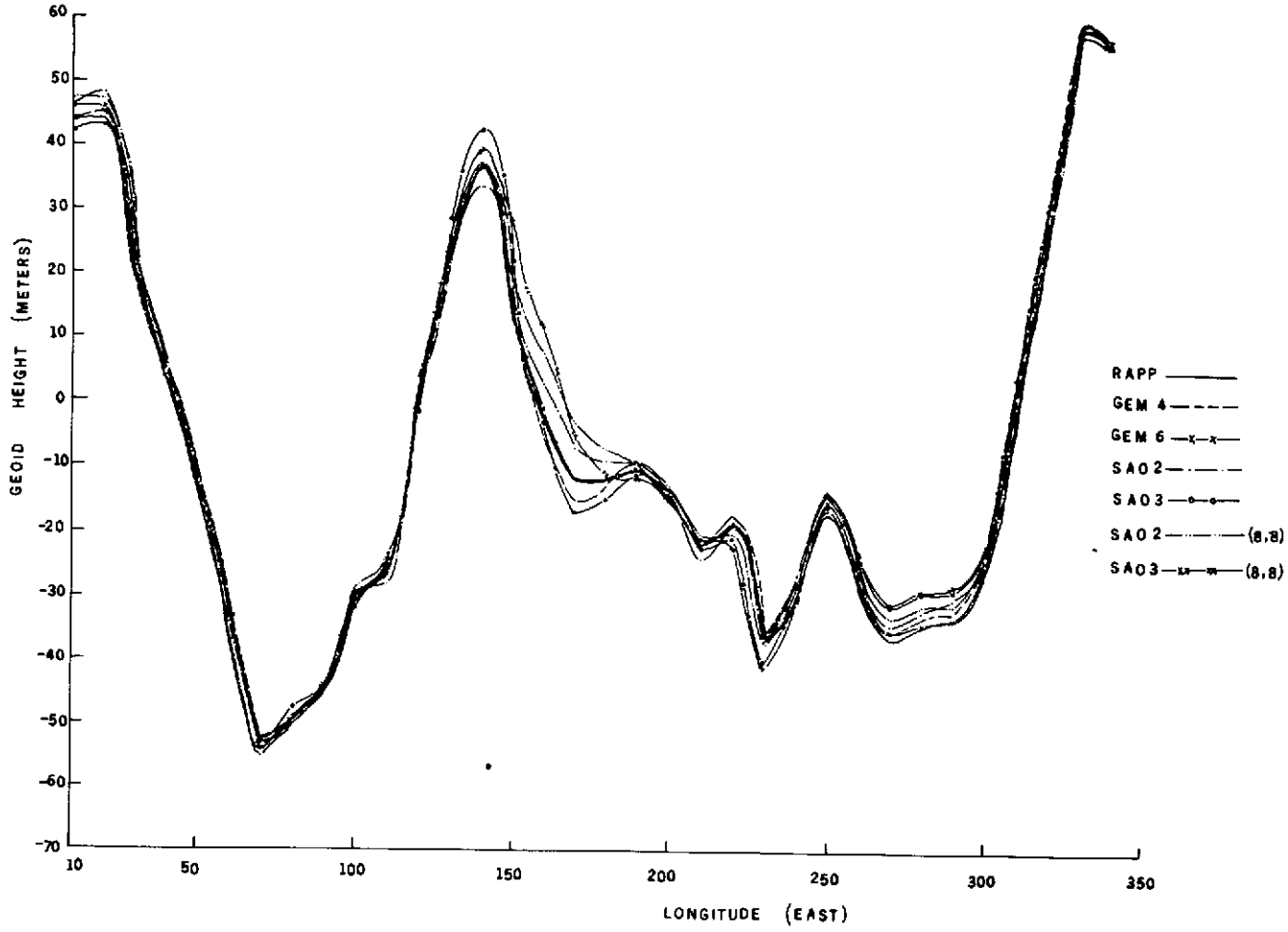

Figure 7. Detailed geoid height profiles at 40°N latitudes based upon the models indicated. The models have been truncated at (12, 12) with the SAO models also truncated at (8, 8). The feature at 175° indicated by the complete SAO-2 model is not present in this figure. Further truncation of the SAO models to (8, 8) had little effect except between 150° and 200° where the profiles moved away from the general trend by as much as 10 meters.

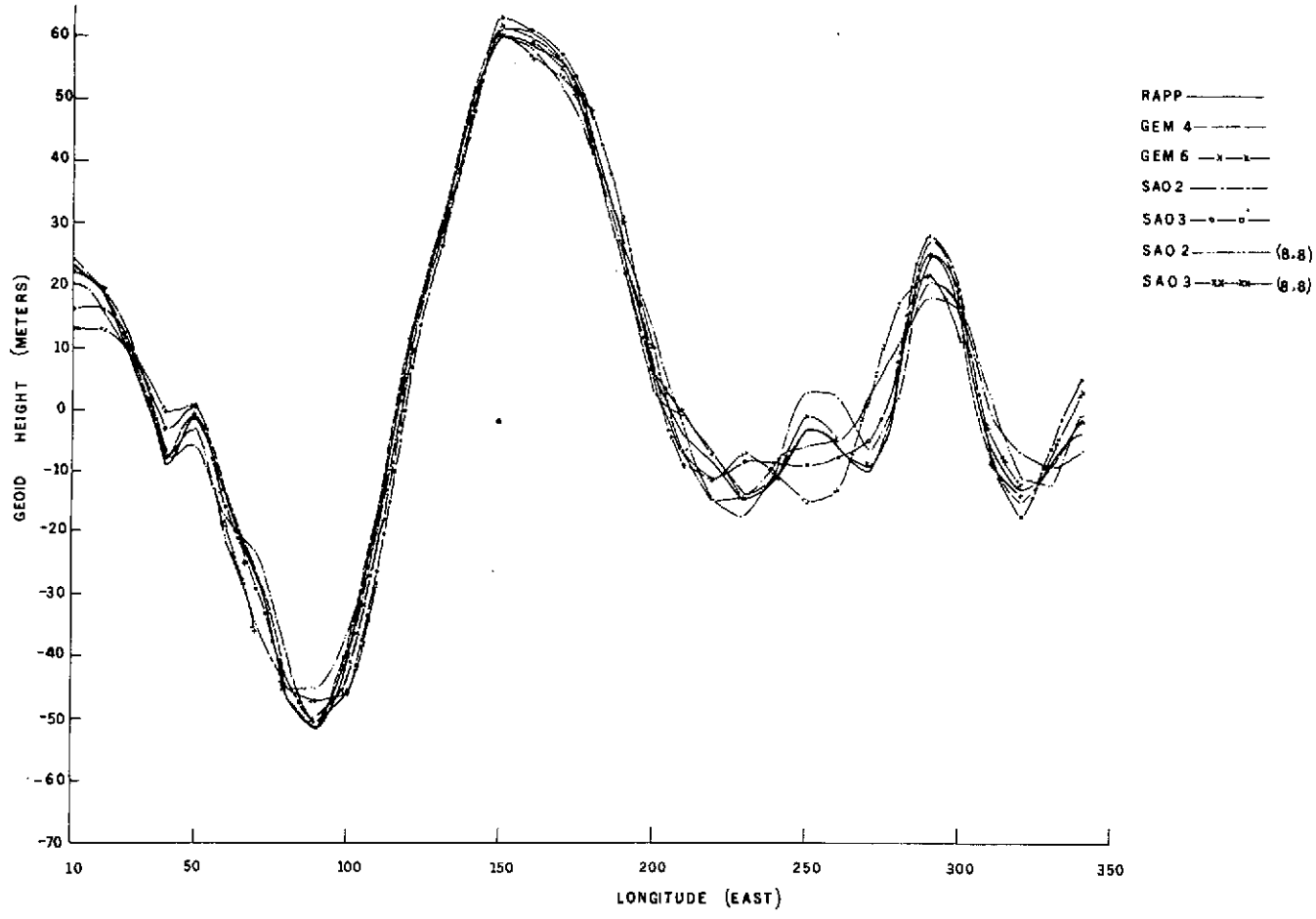

Figure 8. Detailed height profiles at 20°S latitude based upon the models indicated. All models have been truncated at (12, 12) with the SAO models also truncated at (8, 8). The general agreement is better than indicated by the complete models. At 250°, truncated of the SAO-2 model to (8, 8) produced a shift of 10 meters resulting in better agreement with the other models, however, truncation of SAO-3 at (8, 8) resulted in a shift of 10 meters from the general trend.

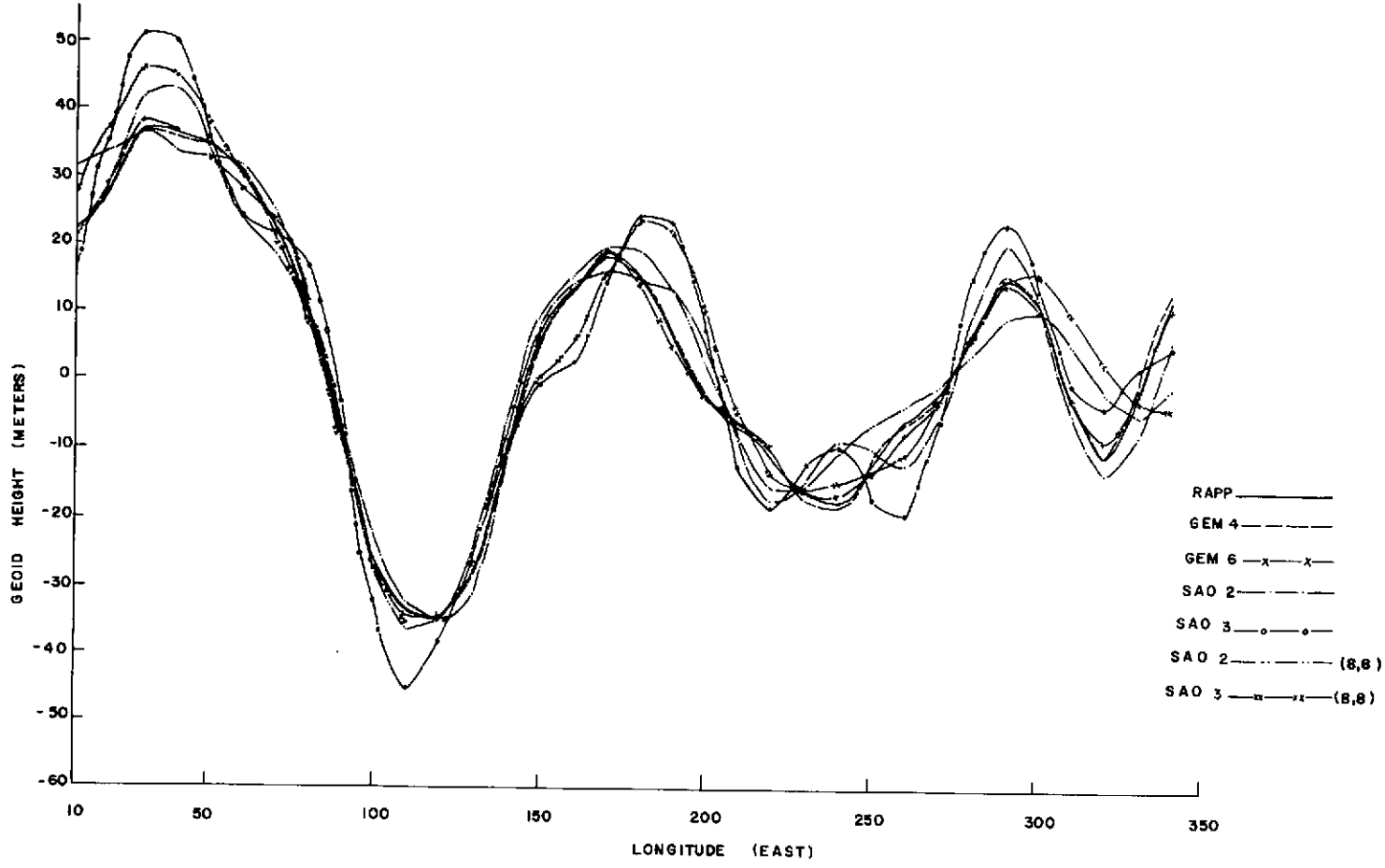

Figure 9. Detailed geoid height profiles at 40°S latitude based upon the models indicated. The models have been truncated at (12, 12) with the SAO models also truncated at (8, 8). The differences are significantly smaller than for the complete models especially in the area of 200° to 275° where now the largest differences are about 10 meters. Truncation of the SAO-3 model at (12, 12) or at (8, 8) did not change the profile at 175° and a shift of about 15° in longitude remains.

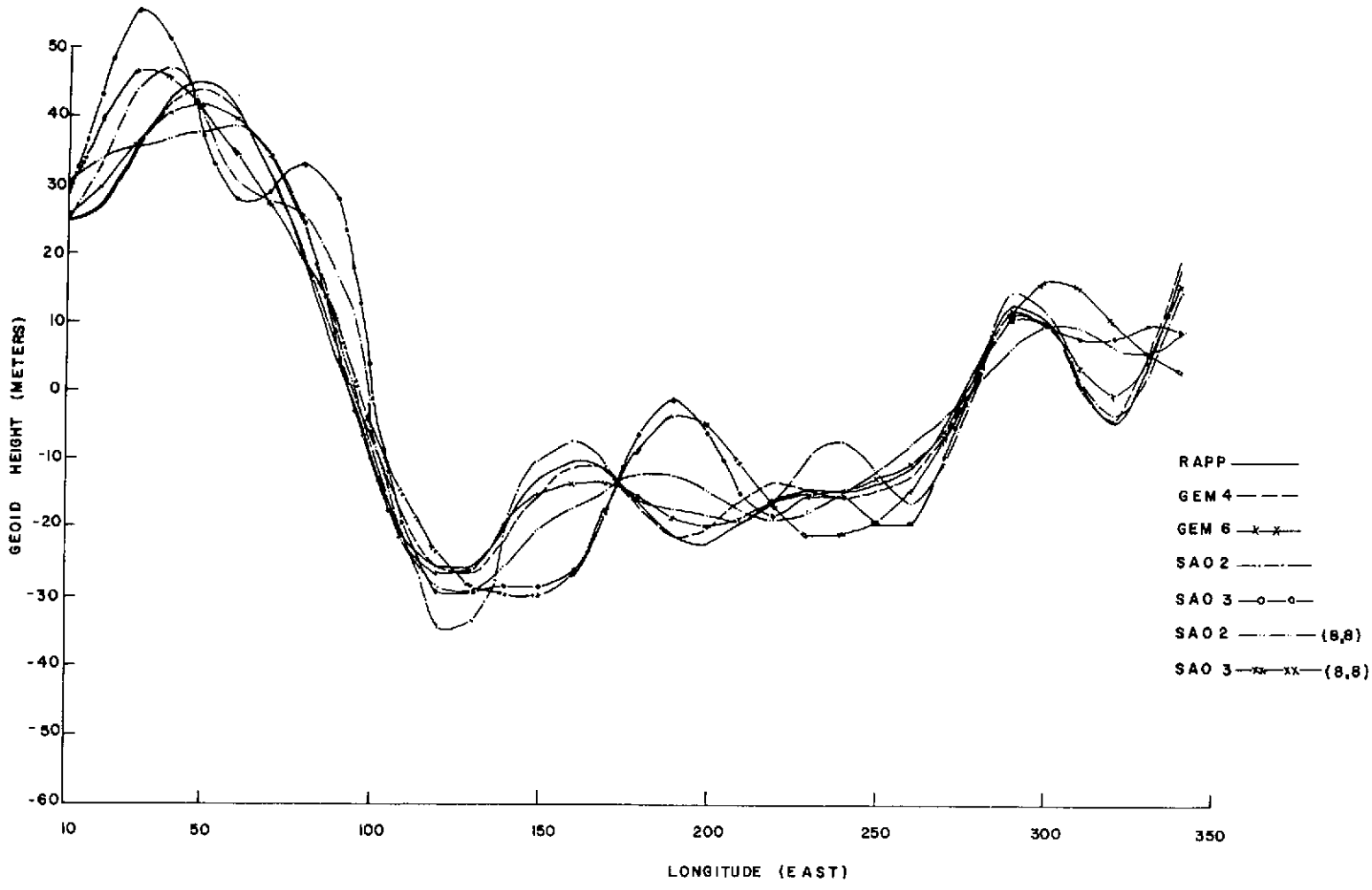

Figure 10. Detailed geoid height profiles at 50°S latitude based upon the models indicated. The models have been truncated at (12, 12) with the SAO models also truncated at (8, 8). The differences have been reduced by the truncation, however variations as large as 20 meters are still noted at 175°.

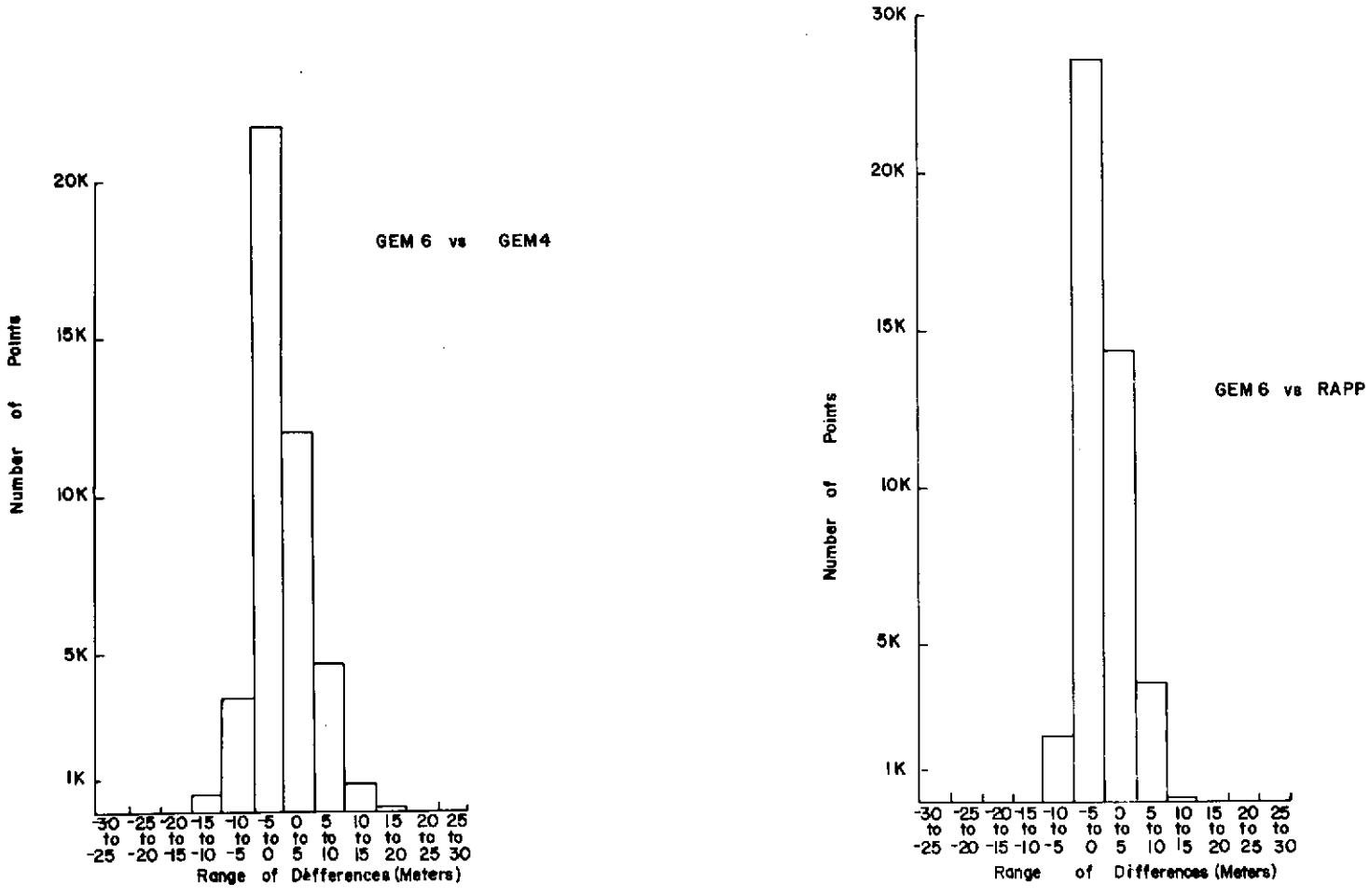

Figure 11. Histograms of differences between the GEM-6 detailed geoid and the GEM-4 and RAPP models. The differences are generally in the range of ± 5 meters.

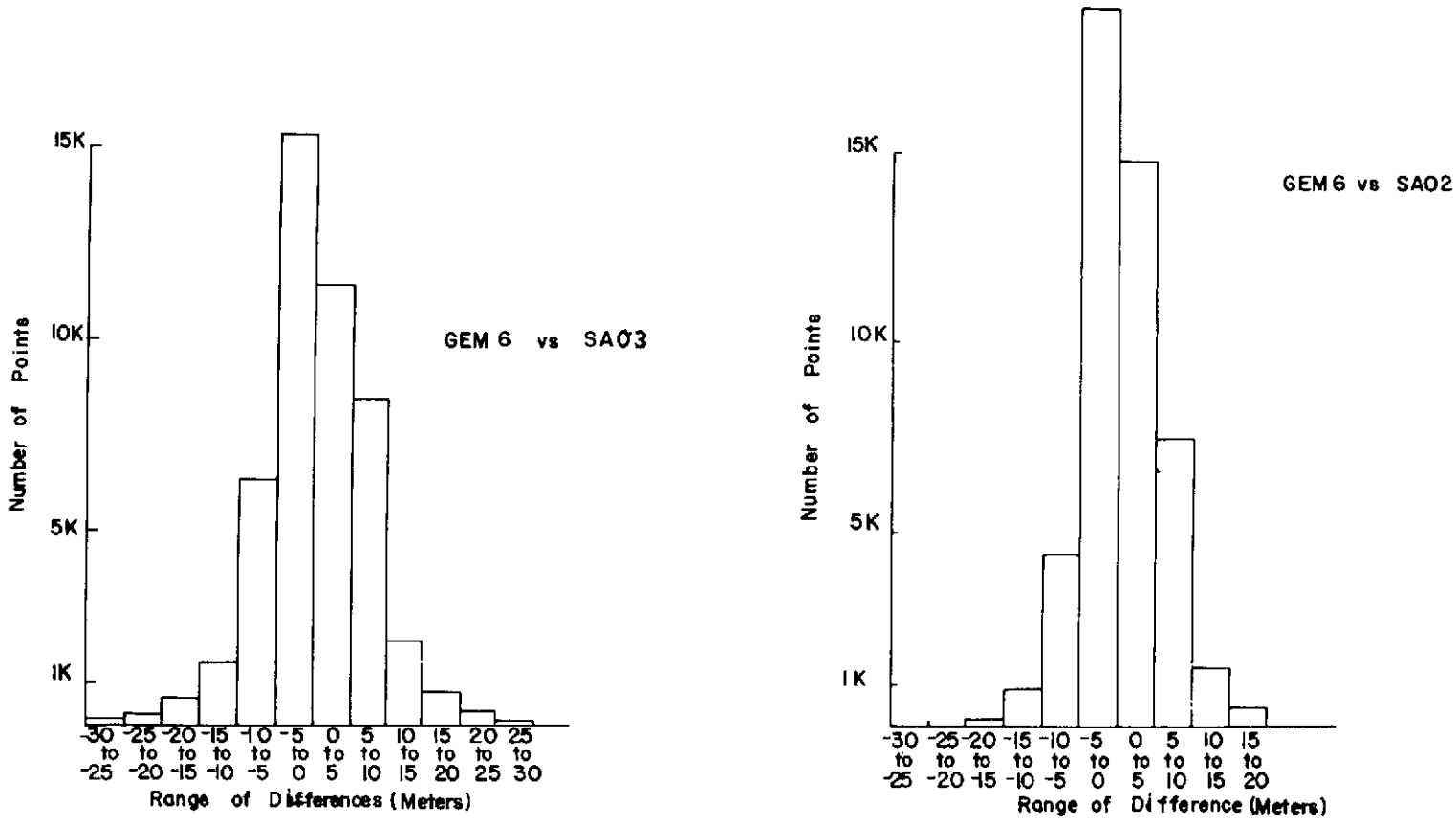

Figure 12. Histograms of differences between the GEM-6 detailed geoid and the SAO-2 and SAO-3 models. The differences are generally in the range of ± 10 meters, however the differences with the SAO-2 model are smaller than the SAO-3 model.

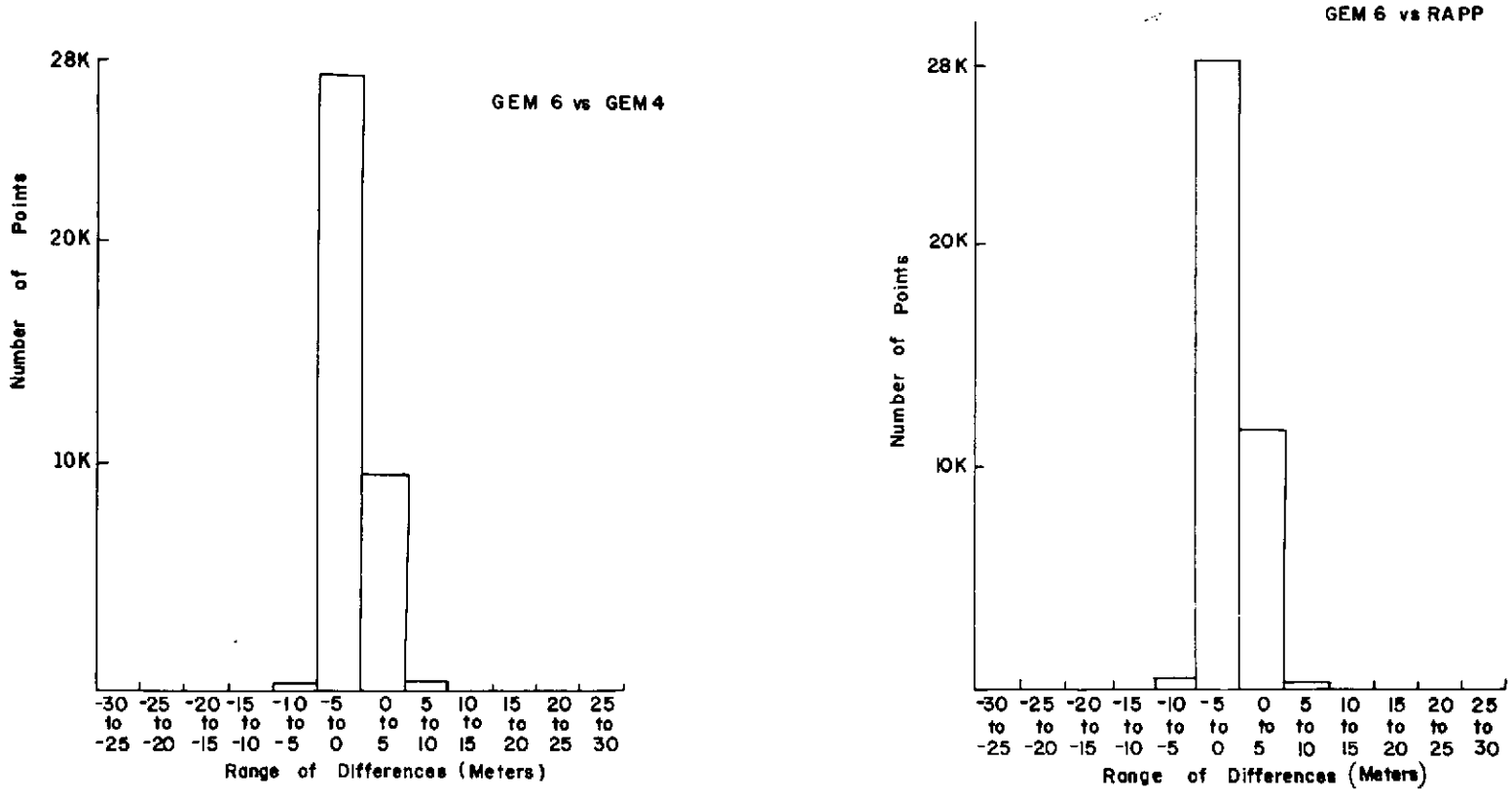

Figure 13. Histograms of differences between the GEM-6 detailed geoid and the GEM-4 and RAPP detailed geoids. All models have been truncated at degree and order 12. The agreement here is significantly better than that indicated in Figure 11 for the complete models. This is attributed to the fact that the coefficients of degree and order less than 12 in the various models are in better agreement than those of degree and order greater than 12.

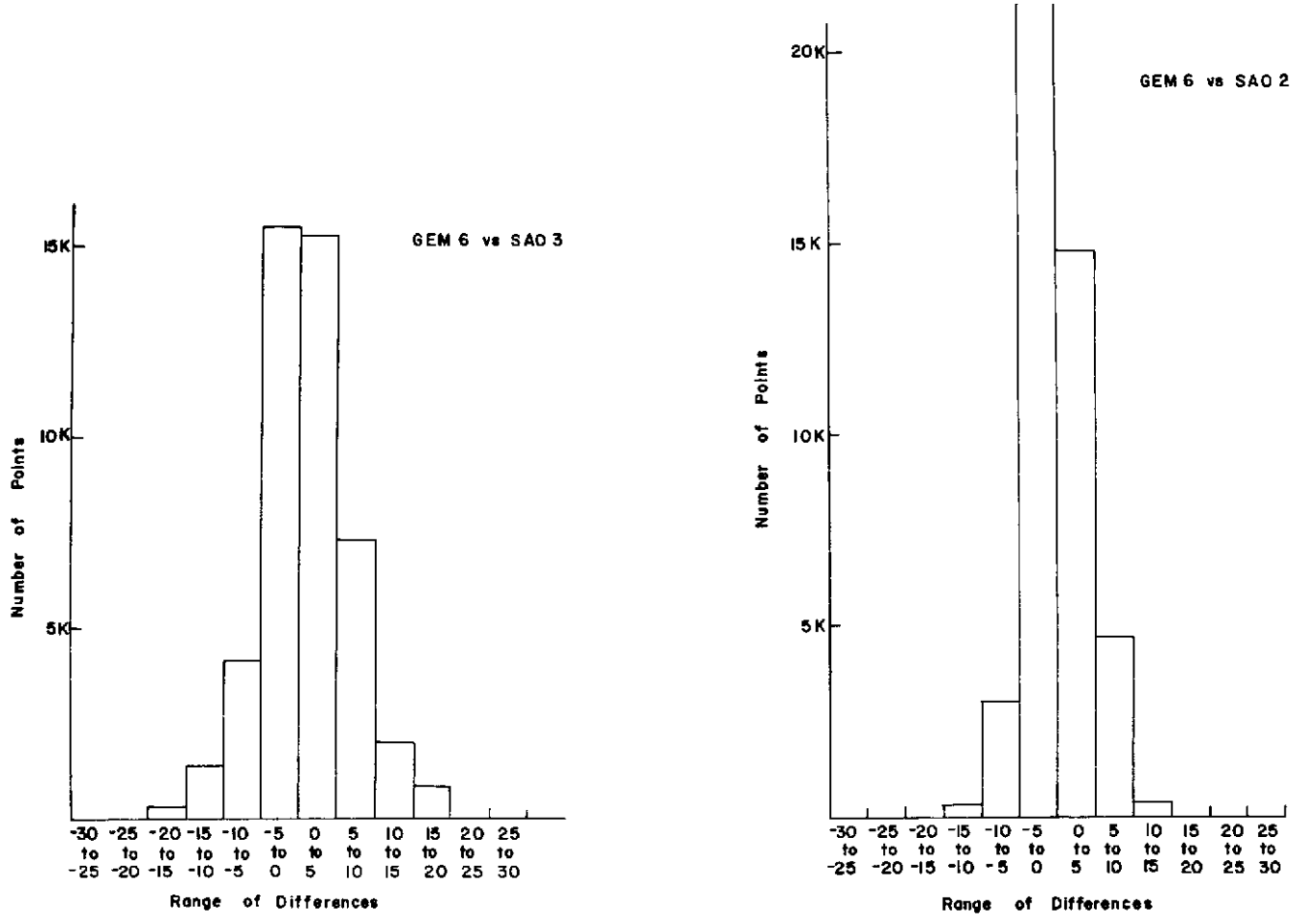

Figure 14. Histograms of differences between the GEM-6 detailed geoid and the SAO-2 and SAO-3 detailed geoid. All models have been truncated at degree and order 12. The agreement here is significantly better than the comparison shown in Figure 12 for the complete models. As noted in Figure 13 this is also attributed to the fact that the coefficients of degree and order less than 12 in the various models are in better agreement than those of degree and order greater than 12.

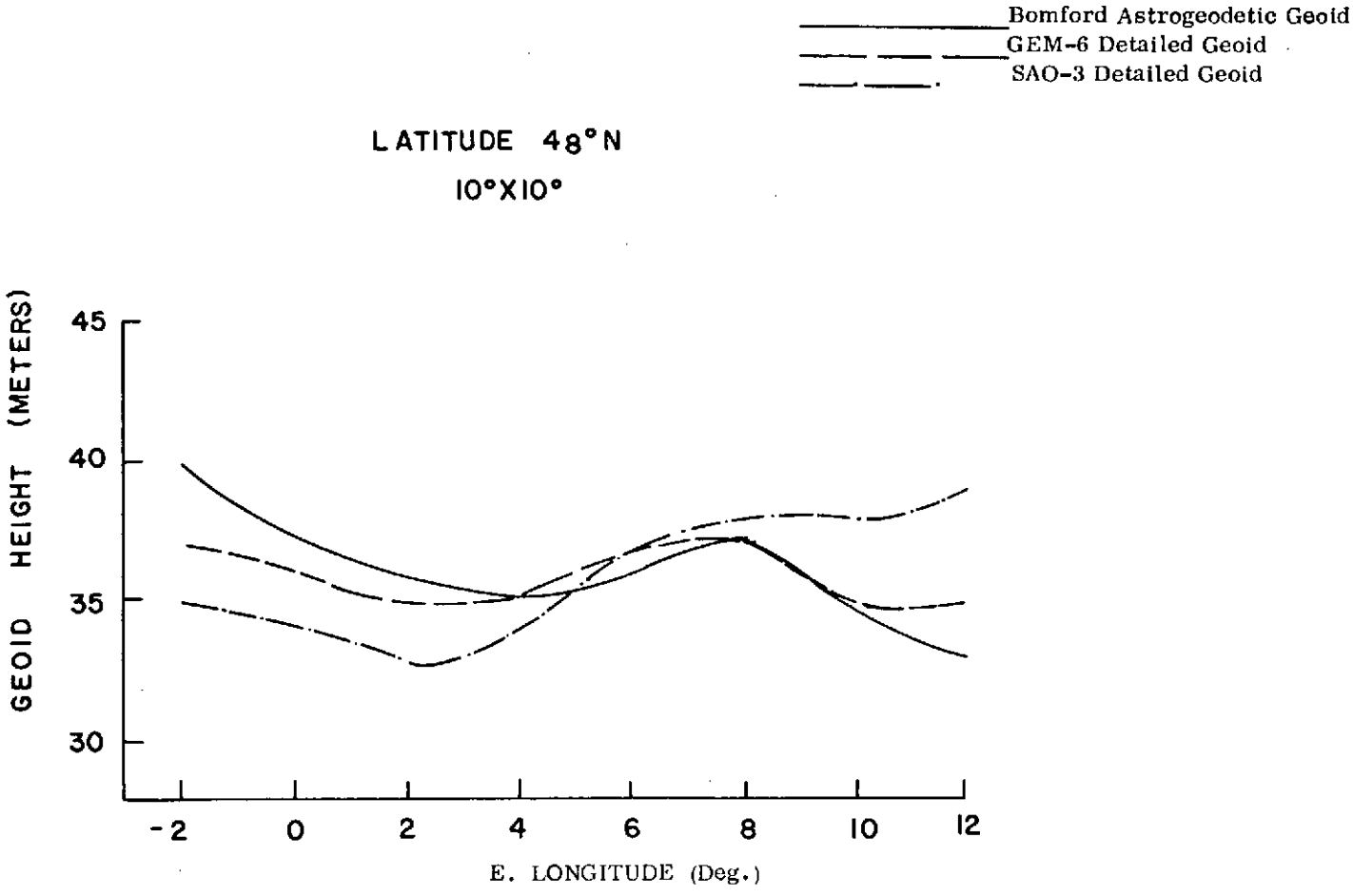

Figure 15. Comparison along a profile at 48°N latitude in Europe between Bomford's astrogeodetic geoid (transformed to a geocentric system) and detailed gravimetric geoids based upon the GEM-6 and SAO-3 models. The gravimetric geoids have been computed using surface data integrated 10° around the computation point. A rotation of about 1.6 arc seconds is noted between the gravimetric geoid based upon the SAO-3 model and Bomford's geoid.

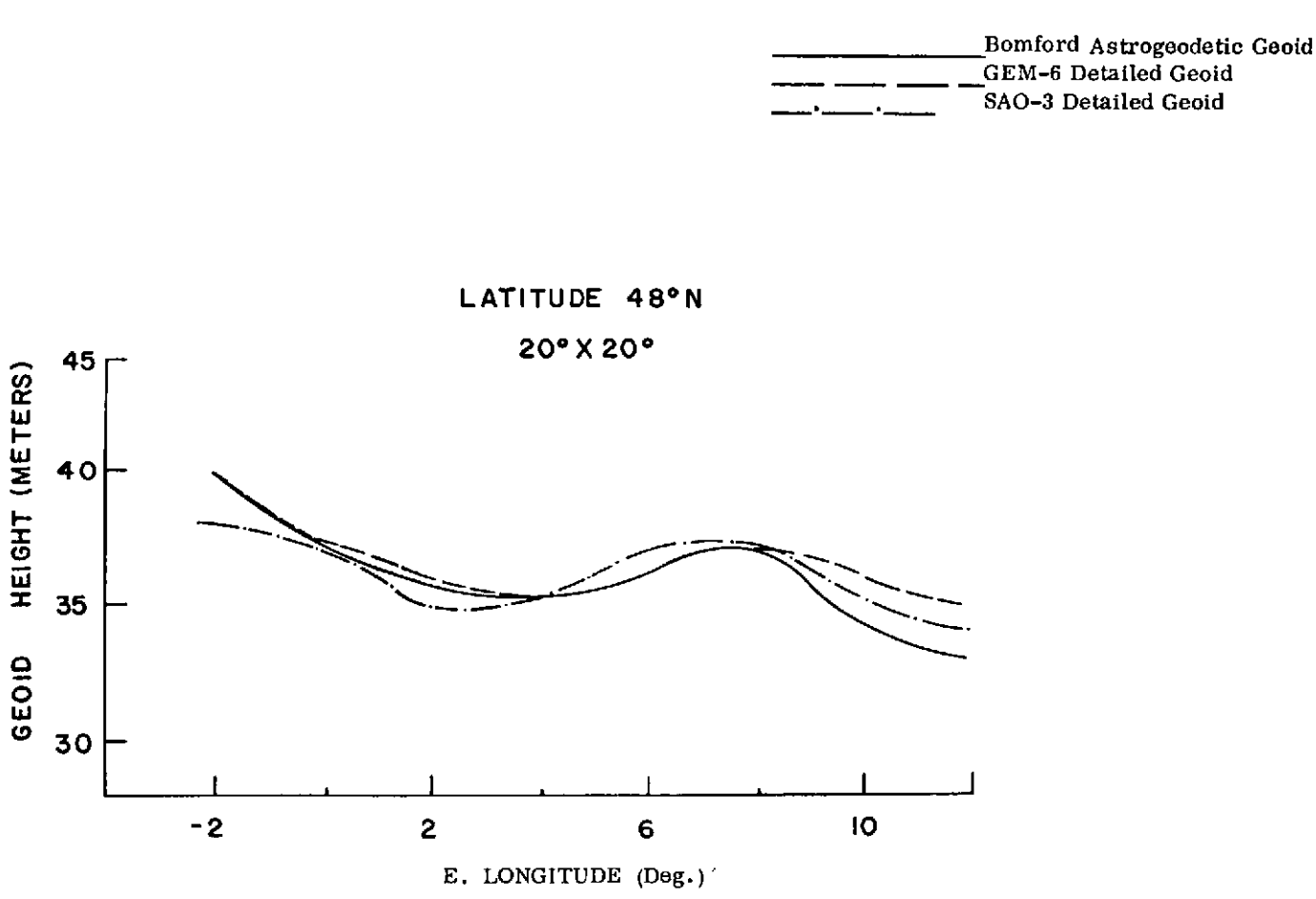

Figure 16. This figure is similar to Figure 15 except that the gravimetric geoids have been computed using surface data integrated 20° around the computational point. The rotation of about 1.6 arc seconds present in Figure 15 between the gravimetric geoid based upon the SAO-3 model and Bomford's geoid was essentially eliminated when the additional surface data were included and now both models agree well with the astrogeodetic geoid. This rotation is attributed to long wavelength errors in the SAO-3 model.

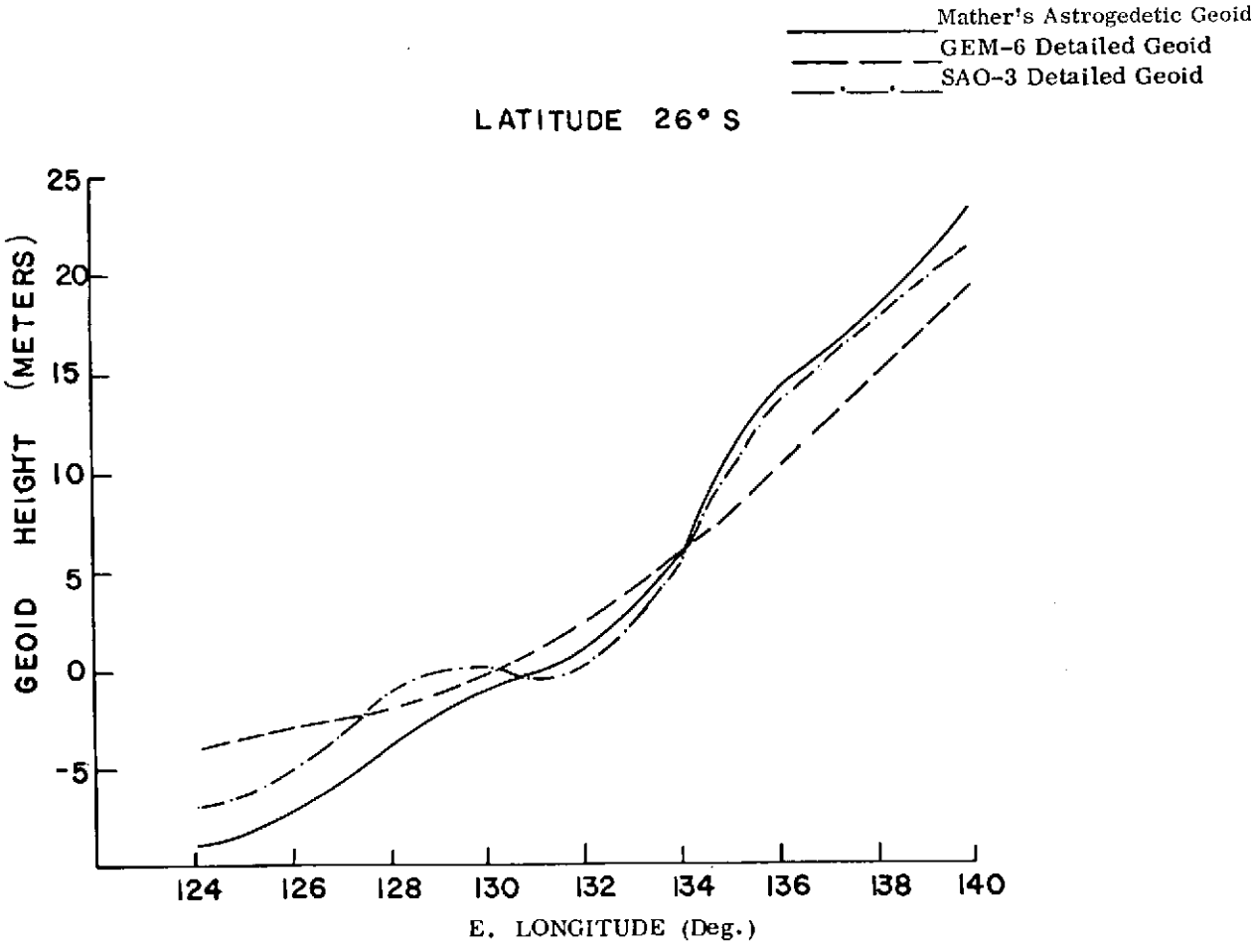

Figure 17. Comparison in Australia along a profile at 26°S latitude between Mather's astrogedetic geoid (transformed to a geocentric reference system) and detailed gravimetric geoids based upon the GEM-6 and SAO-3 models. The gravimetric geoid based upon the SAO-3 model is rotated by about 1 arc second with respect to Mather's geoid, however, the geoid based upon the GEM-6 model is rotated by only about 0.5 arc second, The GEM-6 results agree with those of Mather on the Australian datum.

Table I

Differences between Rice's astrogeodetic geoid and the detailed gravimetric geoids computed using different models. The values have been calculated along a profile at 35°N latitude in the United States. The differences generally lie in the range of ± 2 meters.

E. Long. (deg.)	GEM-4	GEM-6	SAO-II	SAO-III	RAPP
279	-1	-2	-2	-2	-1
277	1	0	0	-2	1
275	-1	-1	-2	-2	-1
273	0	0	-1	-2	0
269	0	1	0	-2	0
268	0	2	0	-1	0
267	-1	1	-1	-1	-1
264	2	3	1	-1	2
261	1	1	0	0	1
259	0	1	0	1	1
255	1	2	2	3	3
253	0	0	0	2	1
250	0	-1	0	2	1
247	0	-1	-1	2	0
245	0	-1	0	1	0
243	2	1	2	2	2

Table II

Comparison between dynamically derived North American Satellite Tracking Station heights (GSFC 1973 solution) and gravimetric geoid heights based upon different models. The values in the table represent $\Delta h = h_{ell} - (hmsl + N)$, where h_{ell} = dynamically determined height of the station above the reference ellipsoid, hmsl = survey height of the station above mean sea level, and N = gravimetric geoid height computed using the models indicated. Differences between the various models are generally less than 3 meters except for the SAO III model in some cases (for example stations 1021, 1042, 7036, 7050).

	Station Number	Lat. (deg)	Long. (deg)	GSFC 73* Long Arc	GEM-4 Meters	GEM-6 Meters	SAO-II Meters	SAO-III Meters	RAPP Meters
Blossom Point, Maryland	1021	38	283	-43	-9	-10	-9	-14	-9
Ft. Myers, Florida	1022	27	278	-29	2	1	-1	-3	1
Goldstone, California	1030	35	243	-30	5	3	2	3	3
St. Johns, Newfoundland	1032	48	307	12	-1	0	5	1	1
East Grand Forks, Minnesota	1034	48	263	-27	1	-1	-3	-3	2
Rosman, North Carolina	1042	35	277	-34	-2	-3	-4	-7	-3
Edinburg, Texas	7036	26	262	-27	-2	-3	-3	-5	-2
Columbia, Missouri	7037	39	268	-35	-1	-1	-2	-6	-1
Bermuda	7039	32	295	-35	4	4	6	2	6
San Juan, Puerto Rico	7040	18	294	-46	4	4	2	3	3
Denver, Colorado	7045	40	255	-18	0	0	1	-2	-1
Greenbelt, Maryland	7050	39	283	-40	-6	-8	-6	-12	-6
Jupiter, Florida	7072	27	280	-32	4	0	-1	-2	1
Sudbury, Canada	7075	46	279	-32	5	5	5	1	6
Organ Pass, New Mexico	9001	32	253	-22	1	1	6	1	2
Mt. Hopkins, Arizona	9021	32	249	-30	-1	-2	-8	-2	-1

*(Marsh, Douglas and Klosko, 1973)